Journal of Alloys and Compounds 818 (2020) 152914

Contents lists available at ScienceDirect

Journal of Alloys and Compounds

journal homepage: http://www.elsevier.com/locate/jalcom

Transition metal ion co-doped MgO–MgF_2-GeO_2:Mn^{4+} red phosphors for white LEDs with wider color reproduction gamut

Hyun Woo Park [a], Hongil Jo [b], Gopinathan Anoop [c], Jae Soo Yoo [a, *]

[a] School of Chemical Engineering and Material Science, Chung-Ang University, Seoul, 06974, South Korea
[b] Department of Chemistry, Sogang University, Seoul, 04107, South Korea
[c] School of Materials Science and Engineering, Gwangju Institute of Science and Technology, Gwangju, 61005, South Korea

ARTICLE INFO

Article history:
Received 2 August 2019
Received in revised form
1 November 2019
Accepted 4 November 2019
Available online 4 November 2019

Keywords:
Mn^{4+} activated red phosphors
MgO–MgF_2-GeO_2
BT.2020
White LEDs
Solid-state lighting

ABSTRACT

Mn^{4+}- activated non-rare-earth based red phosphors are excellent down conversion materials for phosphor-converted light-emitting diode (pc-LEDs) based solid-state lighting applications. However, the low quantum efficiency of Mn^{4+} activated red phosphors under InGaN based blue LED excitation hinders their use in phosphor-converted LEDs. To enhance the absorption at an excitation wavelength of around 420 nm in Mn^{4+}-doped MgO–MgF_2-GeO_2 (MGF: Mn^{4+}), which is a conventional red-emitting lamp phosphor, we doped MGF: Mn^{4+} phosphors with transition metal oxides (Sc_2O_3, Lu_2O_3, Y_2O_3, and La_2O_3) replacing MgO. When excited using 420 nm light, the absorption ratio of the synthesized phosphors with Sc_2O_3 (Sc-MGF:Mn^{4+}) was 58% with an internal quantum efficiency (IQE) of 55% as compared to the 35% IQE of the pristine MGF-Mn^{4+} phosphor. White LEDs were fabricated using Sc-MGF-Mn^{4+} (red), and β-SiAlON:Eu^{2+} (green) on InGaN chips ($\lambda_{em} = 450$ nm) and their performance was compared to the optical performance of LEDs fabricated using K_2SiF_6:Mn^{4+} as the red phosphor. According to the National Television System Committee (NTSC) standard, the color reproduction coverage with an Sc-MGF:Mn^{4+} phosphor-loaded white LED was 121% by the International Commission on Illumination (CIE) 1976, and 80% by the BT.2020 standard. The coverages are 9% and 6% higher than the coverages of LEDs fabricated using K_2SiF_6:Mn^{4+} as the red phosphor according to the NTSC and BT.2020 standards, respectively. Our simple approach to enhance the IQE of Mn^{4+} activated phosphors by co-doping transition metal oxides can be extended to other Mn^{4+} activated phosphor systems for applications that require enhanced absorption, higher luminescent emission intensity, and a wider gamut of color reproduction.

1. Introduction

White light-emitting diodes (WLEDs) are extensively used, not only in general lighting applications, but also as light sources in a variety of electronic devices such as automotive headlights and liquid crystal displays [1,2]. Their applications have now been extended to new fields such as horticulture, micro-displays, and the back-lighting for liquid crystal displays [1,3]. The WLEDs are used in a wide range of applications because of their favorable features such as high luminous efficiency, compactness, long lifespan, low energy consumption, and stability [1–4]. For display applications, a wide gamut of color reproduction is essential to reproduce the color of an object as naturally as possible in the display module [5–10]. Color reproduction standards such as national television systems committee (NTSC), standard red, green blue (sRGB), Adobe RGB, and digital cinema initiatives (DCI) are used to compare the color reproduction gamut of displays. Recently, a new protocol, BT.2020, has been proposed to evaluate the displays that deliver the contents in ultrahigh definition (UHD)—4K and 8K resolution [11,12]. Furthermore, advanced specifications for displays have been proposed for the Tokyo Olympics to be held in 2020. The public broadcaster—Japan broadcasting corporation (NHK) will launch its first official 8K broadcast in 2020. Under these circumstances, color reproduction is becoming more critical, and to expand the color reproduction gamut further, novel phosphors should be developed to meet the color reproduction standard of UHD (8K) displays.

The commercial phosphor-converted WLED technology is based on a combination of an InGaN blue-chip and a yellow phosphor (YAG:Ce^{3+}), which can be excited by blue light having a peak

* Corresponding author.
E-mail address: jsyoo@cau.ac.kr (J.S. Yoo).

https://doi.org/10.1016/j.jallcom.2019.152914
0925-8388/

emission wavelength of 450 nm [13]. Several nitride/oxynitride phosphors with an absorption maximum at 450 nm were developed for white LEDs [3,14–24]. However, blue LED chips and yellow phosphor-based LEDs exhibit a low color rendering index (CRI)—an indicator of accurate color reproduction, because of the lack of a red component in the emitted light. Moreover, such WLEDs composed of a blue LED, and a yellow phosphor do not have a high color temperature for warm-WLEDs. Therefore, developing highly efficient red phosphors has become critical. During the early stages of research on red phosphors, various Eu^{2+} doped nitrides such as $Sr_2Si_5N_8:Eu^{2+}$ and $CaAlSiN_3:Eu^{2+}$were developed [3]. The developed Eu^{2+}-doped silicon-based nitrides and oxynitrides are excellent materials for the fabrication of phosphor-converted WLEDs [3,20,25]. However, utilizing Eu^{2+}-doped silicon-based nitrides in WLEDS presents the following difficulties (1) absorption by Eu^{2+} doped phosphors of wavelengths in the spectral range 400–600 nm, which, consequently, causes serious reabsorption when mixed with the other green or yellow phosphors, (2) broad emission spectra that considerably affect the color reproduction, (3) rare-earth-ions, such as Eu, are highly expensive, and (4) these nitride materials require complicated and expensive synthesizing conditions. To solve these problems, non-rare-earth-based phosphors that emit a sharper and brighter red color were developed, and as part of the solution, considerable efforts have been devoted to the development of non-rare-earth-based red phosphors for use in warm white LEDs [26–32].

Among the various other candidates, less expensive and non-rare-earth Mn^{4+} is a suitable activator for red phosphors because of its narrow absorption spectra (300–480 nm) and lower cost as compared to Eu^{2+} (400–600 nm) [28,33–44]. Numerous studies on Mn^{4+}-doped phosphors such as $MgO–MgF_2-GeO_2:Mn^{4+}$ [45–48], $K_2SiF_6:Mn^{4+}$ [49,50], and other novel phosphors have been reported [2,28]. Among these Mn^{4+} doped phosphors, $MgO–MgF_2-GeO_2:Mn^{4+}$ is a well-known deep red lamp phosphor with a narrow emission width (full-width-at-half maxima (FWHM)–15 nm), and an excitation band located at around 420 nm ($^4A_2 - {}^4T_2$ transitions in Mn^{4+}). For efficient use of the phosphor in WLEDs, the absorption of the phosphor at around 420 nm should be shifted towards the emission wavelength of blue LED—450 nm or enhanced. A feasible strategy by which to achieve the redshift of the excitation spectra is to dope specific octahedral sites in the host material with Mn^{4+} ions. The excitation wavelength can be redshifted by decreasing the crystal field strength because $^4A_2 \rightarrow {}^4T_2$ excitation energy decreases with a decrease in the crystal field strength. It is interesting to note that such a decrease in the crystal field strength will not alter the emission wavelength because the energy related to the $^2E \rightarrow {}^4A_2$ transition is nearly independent of the crystal field strength. Previous studies have attempted to improve the optical characteristics of the phosphors by changing the reaction conditions, and Nichia Corp, Japan, has a patent (US 2015/0349,213 A1) on these techniques.

In this study, experiments were conducted to synthesize a $MgO–MgF_2-GeO_2:Mn^{4+}$ ($MGF:Mn^{4+}$) phosphor with enhanced absorption at 420 nm. We have developed a strategy that involves replacing MgO with other metal oxides to improve the absorbance at around 420 nm. The white LEDs were then fabricated by coating InGaN chips ($\lambda_{em} = 450$ nm) with synthesized phosphors and β-SiAlON:Eu^{2+}. We analyzed the optical characteristics of the white LEDs in terms of their color reproduction gamut. We also demonstrated the variation from the International Telecommunication Union's (ITU) BT.2020 recommendation (color production region) in the WLED application due to the use of our $MgO–MgF_2-GeO_2:Mn^{4+}$ phosphor. Further, the variations in the BT.2020 coordinates were compared with those of the WLEDs fabricated using the $K_2SiF_6:Mn^{4+}$ red phosphor.

2. Experimental

2.1. Synthesis of red-emitting $MgO–MgF_2-GeO_2$ phosphor

The solid-state reaction method was used to synthesize the red phosphor. The starting materials for synthesizing $MGF:Mn^{4+}$were MgO, MgF_2, GeO_2, and Mn_2O_3 and metal oxide A_2O_3 (A: Sc, Lu, Y, La). Initially, appropriate proportions of the raw materials were blended in isopropyl alcohol at room temperature and were then dried in an oven at 100 °C. Next, the mixture was transferred into an alumina crucible, loaded into a furnace, and sintered at 1100 °C for 5 h in air. The samples were cooled down to room temperature to obtain the phosphors.

2.2. Characterization

The prepared phosphor was analyzed by powder X-ray diffraction (XRD) (D8 Advance, Bruker, Germany) at the wavelength of Cu Kα-radiation to identify its phase and crystal structure. The room temperature photo-luminescent emission (PL) and excitation (PLE) spectra were recorded using a xenon lamp (PSI, Korea). The ratio of absorption and the quantum efficiency were measured using a $BaSO_4$-coated integrating sphere with a photomultiplier tube and a xenon lamp (PSI, Korea). The temperature-dependent PL characteristics of the samples were examined using a Hitachi F-7000 at different temperatures ranging from 25 to 200 °C.

2.3. Fabrication of phosphor-converted white LEDs

The phosphor-converted white LEDs were fabricated by coating the set of phosphors, Sc-$MGF:Mn^{4+}$, and β-SiAlON:Eu^{2+} (green-emitting phosphor) on the 450 nm blue-emitting chip. The ratios of the phosphors to the silicone resin, and of the green to the red phosphors were adjusted to obtain the proper white point. The pressure and duration of the drop were controlled with a dispenser. The correlated color temperature of the white point of the white LED was set to 10,000 K. In this process, the bubbles of the epoxy composite were removed using a de-foamer. Finally, the packaged LED was cured at 150 °C to harden the silicone resin added with the phosphors.

3. Results and discussion

In $MGF:Mn^{4+}$, the Mn^{4+} ions that occupy octahedral sites usually emit red light [51]. Because of similar ionic radii and charge balances, Mn^{4+} ions are likely to substitute for Ge^{4+} sites even though octahedral Mg^{2+} sites are also available for substitution. The replacement of MgO with a small amount of other metal oxide was carried out to create the right conditions so that Mn^{4+} could occupy the specific Ge^{4+} sites rather than the Mg^{2+} sites. The XRD patterns of the as-synthesized MGF: Mn^{4+}phosphor, and Sc_2O_3 substituted phosphor are shown in Fig. 1(a) and (b), respectively, and they closely match with the crystal structure of $Mg_{14}Ge_5O_{24}$ (ICSD-9371). However, note that our raw materials consist of MgF_2 and therefore, our $MgO–MgF_2-GeO_2:Mn^{4+}$ phosphor will contain F ions and other related impurities. The XRD analysis suggests that the $MGF:Mn^{4+}$ phosphor synthesized in the present study is isostructural with $Mg_{14}Ge_5O_{24}$.

Fig. 2a shows the emission and excitation spectrum of the as-synthesized MGF: Mn^{4+}phosphor. It has an excitation band of around 420 nm due to the $^4A_2 \rightarrow {}^4T_2$ transition and emits a sharp (FWHM ~15 nm) band at 658 nm due to a $^2E \rightarrow {}^4A_2$ transition. The most popular method of fabricating a white LED is to use a 450 nm-emitting chip as the exciting light source, because it is the most efficient light source, and further, it is a part of the primary color

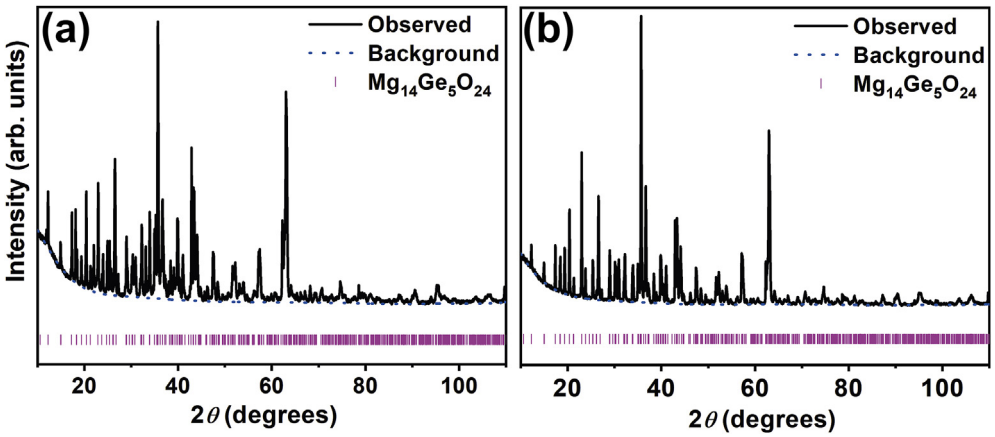

Fig. 1. XRD patterns of (a) as-synthesized MgO–MgF_2-GeO_2:Mn^{4+} phosphor and (b) MgO–MgF_2-GeO_2:Mn^{4+} phosphor synthesized with Sc_2O_3.

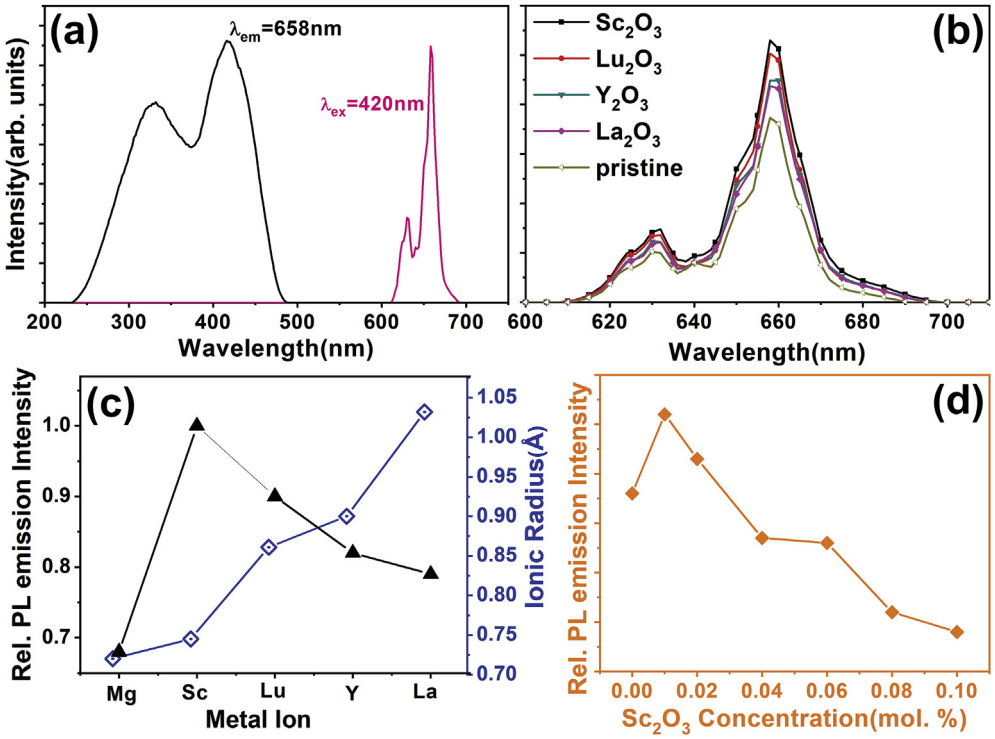

Fig. 2. (a) Excitation and emission spectra of MgO–MgF_2-GeO_2:Mn^{4+} phosphor (b) Emission spectra (λ_{ex} = 420 nm) of MgO–MgF_2-GeO_2:Mn^{4+} phosphor synthesized with different components (Sc_2O_3, Lu_2O_3, Bi_2O_3, Ga_2O_3,Y_2O_3, none) (c) Relative intensity graph of MgO–MgF_2-GeO_2:Mn^{4+} phosphor synthesized with different components (Sc_2O_3, Lu_2O_3, Y_2O_3, La_2O_3) and ionic radius (Sc, Lu, Y, La) and (d) Relative intensity plot according to different Sc_2O_3 concentrations (molar ratio).

(blue light). However, from Fig. 2a, it is apparent that the absorption of the MGF:Mn^{4+} phosphor around 450 nm is relatively low.

On the other hand, the MGF:Mn^{4+} phosphor has deep red narrow-band light emission that favors a wider gamut of color reproduction. Therefore, an improvement in the luminescence intensity of the phosphor is possible if Mn^{4+} occupies the Ge sites of a given structure. Previous studies have shown that the use of SrF2 as a flux, among other fluoride compounds, is the most efficient method to produce materials with good optical properties.18,19 To achieve excellent optical characteristics, Mn^{4+} should occupy octahedral sites, and the synthesized phosphors' hosts should provide suitable sites for the replacement. As mentioned earlier, Mn^{4+} ions can occupy both the Mg^{2+} and Ge^{4+} sites of the octahedral structure, resulting in a deep red light. To begin with, the partial substitution of the Mg ion by various other metal ions was attempted in our experiments to examine variation in the luminescence intensity. We used metal oxides such as Sc_2O_3, Lu_2O_3, Y_2O_3, and La_2O_3. The PL intensities of the MGF:Mn^{4+} phosphor doped with Sc_2O_3, Lu_2O_3, Y_2O_3, and La_2O_3 are shown in Fig. 2b.

As expected, substantial enhancements were observed in the luminescence intensity, as shown in Figs: 2b and 2d. The partial substitution of Mg ions by Sc ions significantly affects the luminescence emission intensity. Therefore, a partial substitution of Mg with Sc results in the substitution of more Mn^{4+} at the octahedral Ge^{4+}, thus improving the optical characteristics, especially the absorption. Therefore, further experiments were carried out to investigate the effect of Sc_2O_3 on the host crystal structure and the luminescence intensity. It is assumed that the reasons for this

behavior are the substitution of trivalent metal oxides and their ionic sizes. Initially, when a small amount of trivalent element substituted for Mg, it helped in the oxidation of the Mn ion and led the Mn^{4+} ion to occupy a Ge1 site.[32] Furthermore, the emission probability strongly depended on the local structure around the Mn^{4+} ions. The incorporation of Sc reduced the probability of Mn^{4+} occupying Mg^{2+} sites, which resulted in an enhancement in the red emission. Therefore, we presume that the enhanced luminescence is because of the Mn^{4+} doped at the Ge^{4+} octahedral sites in the MgO−MgF_2-GeO_2 host lattice. Moreover, it is essential that Mn^{4+} in the MgO−MgF_2-GeO_2 host should occupy octahedral sites of Ge^{4+} ions. Because of this occupation, the phosphors prepared by adding the trivalent metal oxide exhibited higher luminance than did pristine phosphor. Additionally, Sc_2O_3 substitution led to the maximum improvement, presumably because Sc and Mg had similar ionic radii (Mg ionic radius is 0.72 Å, and Sc ionic radius is 0.745 Å). Therefore, Sc substitution reduces the probability of Mn^{4+} occupation at Mg^{2+} sites. However, when the ionic radius of the substituting ion is much higher than the ionic radius of Mg^{2+}, the luminescent emission intensity decreases because the larger ions such as Lu, Y, and La can occupy off-center sites. A comparison of the ionic radii and relative intensities is shown in Fig. 2c.

In order to find the optimum Sc concentration, the concentration of Sc_2O_3 was varied from 0 to 0.1 M ratios. As shown in Fig. 4, the light emission intensity reaches a maximum when the molar ratio of Sc was 0.01, and a further increase in Sc concentration decreased the PL emission intensity.

Fig. 3a and its inset show the spectra of photoluminescence (PL) and excitation (PLE) of the MGF:Mn^{4+} phosphor doped with 0.01 mol.% Sc_2O_3. The partial substitution of Mg ions by Sc ions obviously improves the emission and excitation. The absorption ratio and the IQE (η_i) were calculated by the following equation [1]:

$$\eta_i = \frac{\int \lambda \cdot P(\lambda) d\lambda}{\int \lambda \{E(\lambda) - R(\lambda)\} d\lambda} \quad (1)$$

where E(λ)/hν, R(λ)/hν, and P(λ)/hν are the number of photons in the spectra of excitation, reflectance, and emission of the phosphor, respectively. The measured absorption ratio over the range from 400 to 500 nm of the sample synthesized by the conventional method and by partial replacement was 54% and 58%, respectively. The IQE values were 35% for the as-synthesized phosphor and 55% for the MGF:Mn^{4+} phosphor replaced with 0.01 mol.% Sc_2O_3. The absorption ratio and the IQE were substantially enhanced by 4% and 20%, respectively. The addition of Sc was found to be highly beneficial in achieving an enhanced luminescence from the MGF:Mn^{4+} phosphor.

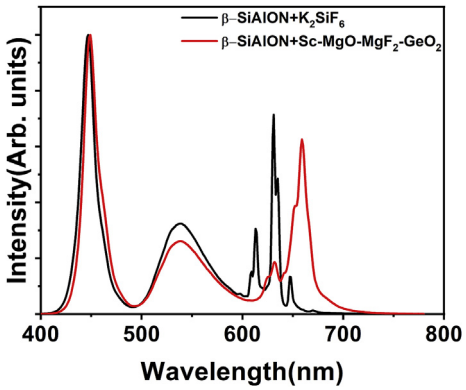

Fig. 4. Emission spectra of two different phosphor-converted white LEDs. (Red phosphors: K_2SiF_6:Mn^{4+} and Sc-MGF:Mn^{4+}) (Green phosphor: β-SiAlON:Eu^{2+}, in common). (For interpretation of the references to color in this figure legend, the reader is referred to the Web version of this article.)

The thermal behavior of the phosphor is very critical from the perspective of the device application. As shown in Fig. 3b, the temperature-dependent PL intensity of the MGF:Mn^{4+} phosphor does not show a significant degradation with temperature. The outstanding thermal stability of the MGF:Mn^{4+} phosphor is because of its stable structure wherein Mn^{4+} ions are well-trapped at the octahedral Ge^{4+} sites. The Sc incorporated MGF:Mn^{4+} phosphor exhibits much better thermal stability up to 200 °C than does the pristine MGF:Mn^{4+} phosphor, which once again suggests that the addition of Sc was beneficial in achieving high luminescent intensity as well as thermal stability. Furthermore, the Sc substitution of Mg in MGF:Mn^{4+} has enhanced the PL excitation at a wavelength of around 420 nm, and the IQE. Note that the FWHM of the emission spectra was not much affected by the Sc substitution.

In order to investigate the feasibility of MGF:Mn^{4+} phosphors incorporated with Sc in solid-state lighting, we fabricated WLEDs by coating the Sc-MGF:Mn^{4+} phosphor (red) and β-SiAlON:Eu^{2+} (green) on InGaN chips (λ_{em} = 450 nm). The fabricated white LEDs were then compared with the WLEDs fabricated using K_2SiF_6:Mn^{4+} as red phosphor, instead of Sc-MGF:Mn^{4+}. Fig. 4 shows the emission spectra of the white LEDs obtained by using the two different types of red phosphors.

The optical properties and color reproduction of the two white LEDs are compared in Table 1. The Sc-MGF:Mn^{4+} phosphor

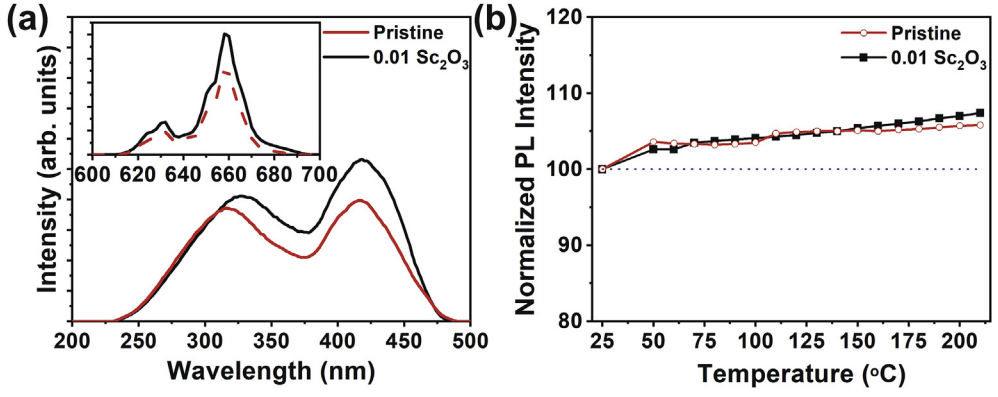

Fig. 3. (a) Excitation spectra (λ_{em} = 658 nm) of MgO−MgF_2-GeO_2:Mn^{4+} phosphor synthesized with Sc_2O_3 and without Sc_2O_3 (b) Emission spectra (λ_{ex} = 420 nm) of MgO−MgF_2-GeO_2:Mn^{4+} phosphor synthesized with Sc_2O_3 and without Sc_2O_3. Temperature dependence of PL intensities (λ_{ex} = 420 nm) of pristine and Sc-MgO-MgF_2-GeO_2:Mn^{4+} phosphors.

Table 1
Optical properties of white LEDs fabricated with two red phosphors.

Phosphor		Luminous Flux (lm)	CIE 1931 (x. y)	Coverage (%)		CIE 1976 (u′, v′)	Coverage (%)	
Green	Red			NTSC	BT.2020		NTSC	BT.2020
β-SiAlON:Eu^{2+}	K_2SiF_6:Mn^{4+}	6.24	(0.26,0.27)	95	71	(0.19,0.43)	112	74
	Sc-MGF:Mn^{4+}	3.27	(0.25,0.24)	98	73	(0.19,0.40)	121	80

generates high-purity deep red color at 658 nm from the narrow FWHM of ~15 nm. The K_2SiF_6:Mn^{4+} also emits high-purity deep red color at 630 nm, with a narrow bandwidth. Note that the Sc-MGF:Mn^{4+} phosphor has a lower absorption at 450 nm than that of K_2SiF_6:Mn^{4+} and, therefore, the luminous flux of the WLEDs fabricated using Sc-MGF:Mn^{4+} phosphor is nearly half that of the luminous flux of the WLEDs fabricated using K_2SiF_6:Mn^{4+}. However, white LEDs manufactured using the MGF:Mn^{4+} phosphor exhibit superior color reproduction coverage (Table 1 and Fig. 5). Basically, by the NTSC standard, the coverage of color reproduction with the K_2SiF_6:Mn^{4+} phosphor-loaded white LED is 95% in CIE1931 and 112% in CIE1976, while with the Sc-MGF:Mn^{4+} phosphor-loaded white LED, the coverage was enhanced to 98% in CIE1931 and 121% in CIE1976 coordinate systems. Moreover, to analyze the color reproduction coverage of the LEDs further, the coverages based on the BT.2020 standard used for UHD (ultrahigh definition) displays were evaluated. From the BT.2020 protocol, the coverage of color reproduction with the K_2SiF_6:Mn^{4+} phosphor-loaded white LED is 71% in CIE1931 and 74% in CIE1976, while that for the MGF phosphor-loaded white LED was enhanced to 73% in CIE1931 and 80% in CIE1976.

Further analyses of the fabricated LEDs were carried out using the TM-30 standard.

Instead of the conventional color rendering indices comprised of 16 points, the TM-30 standard uses 99 color samples to analyze the color rendering indices [52,53]. Fig. 6(a and c) show the color sample fidelity and the local color fidelity for the 16 hue angle bin for both WLEDs fabricated using the Sc-MgO-MgF_2-GeO_2:Mn^{4+} red

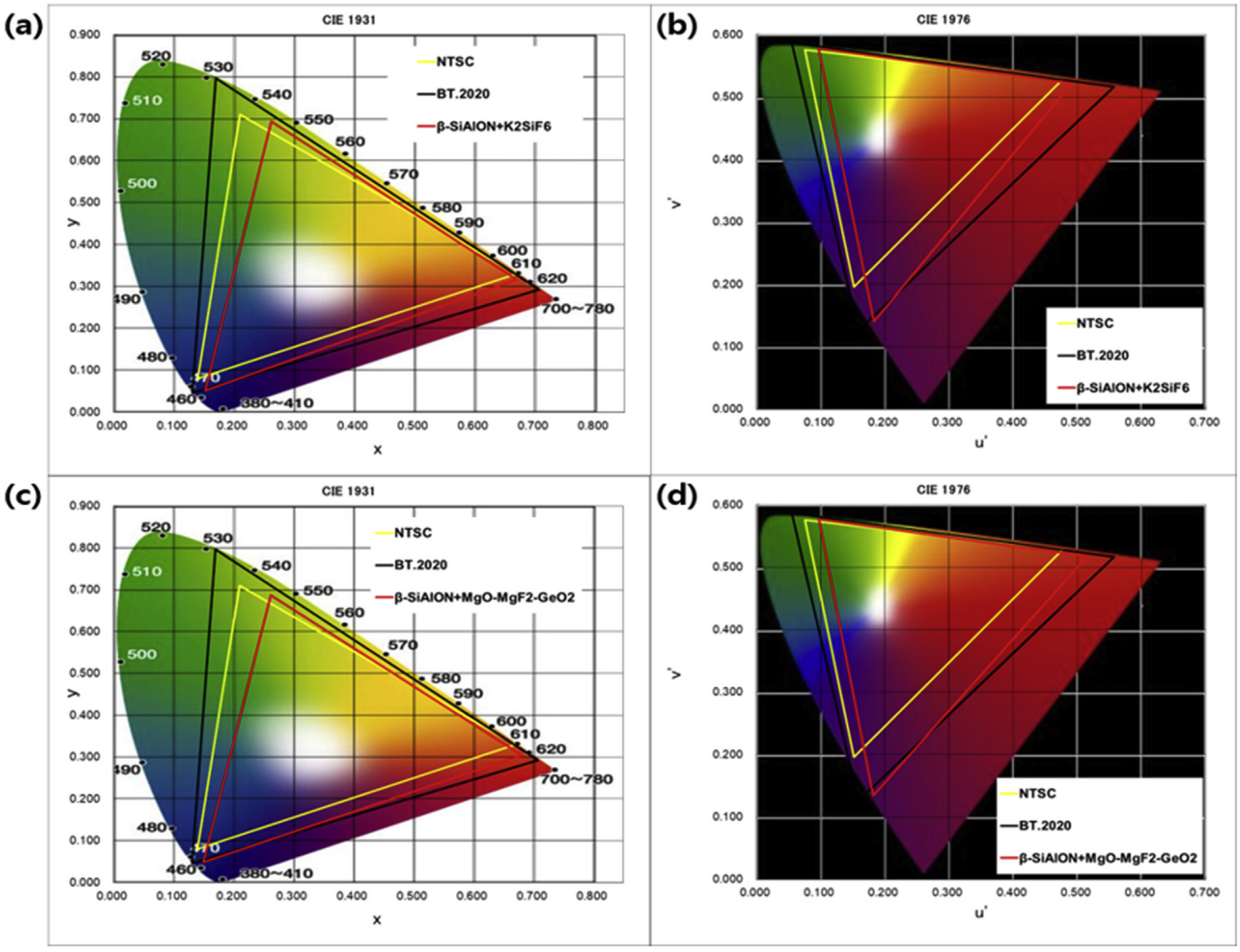

Fig. 5. (a) CIE 1931 chromaticity coordinates of white LED with blue-chip (450 nm), β-SiAlON:Eu^{2+}(green), K_2SiF_6:Mn^{4+}(red) phosphors (b) CIE 1976 chromaticity coordinates of white LED with blue-chip (450 nm), β-SiAlON:Eu^{2+}(green), K_2SiF_6:Mn^{4+}(red) phosphors (c) CIE 1931 chromaticity coordinates of white LED with blue-chip (450 nm), β-SiAlO-N:Eu^{2+}(green), Sc-MGF:Mn^{4+} (red) phosphors (d) CIE 1976 chromaticity coordinates of white LED with blue-chip (450 nm), β-SiAlON:Eu^{2+}(green), Sc-MGF:Mn^{4+} (red) phosphors. (For interpretation of the references to color in this figure legend, the reader is referred to the Web version of this article.)

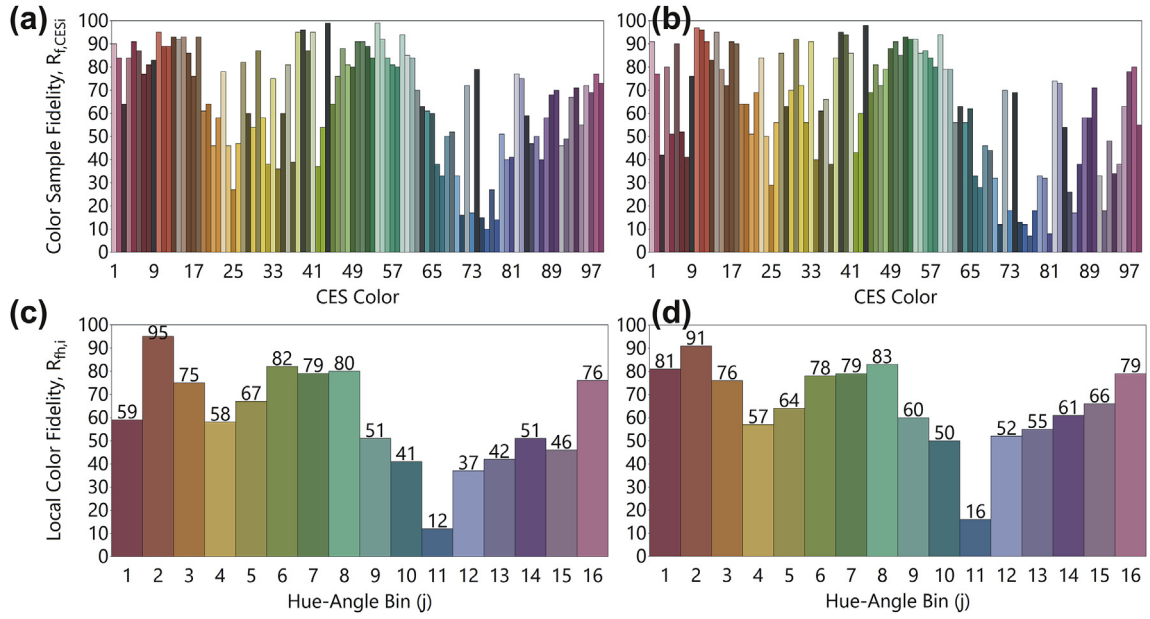

Fig. 6. (a,c) the color sample fidelity and local color fidelity of WLEDs fabricated using β-SiAlON:Eu^{2+}(green), Sc-MGF:Mn^{4+} (red) phosphors. (b and d) the corresponding plot of the WLEDs fabricated using β-SiAlON:Eu^{2+}(green), K_2SiF_6:Mn^{4+}(red) phosphors. (For interpretation of the references to color in this figure legend, the reader is referred to the Web version of this article.)

phosphor, while Fig. 6 (b and d) show the corresponding plots of the WLEDs fabricated using the K_2SiF_6: Mn^{4+}-red phosphor. The fabricated LEDs exhibit excellent color sample fidelity, as well as local color fidelity, which once again suggests that our Sc-MGF:Mn^{4+} red phosphor exhibits color reproduction characteristics very similar to that of the K_2SiF_6:Mn^{4+} phosphor.

The color reproduction gamut of the fabricated LEDs was analyzed further using the TM-30 standard, whose gamut plots are shown in Fig. 7. Fig. 7a and b depict the gamut area of the WLEDs fabricated using Sc-MGF:Mn^{4+} and K_2SiF_6:Mn^{4+} red phosphors.

The black lines in the plot show the gamut of a standard source while the red lines correspond to the gamut area of the fabricated LEDs using Sc-MGF:Mn^{4+} and K_2SiF_6:Mn^{4+} red phosphors. Again, our Sc-MGF:Mn^{4+} exhibits a slightly wider gamut area compared to the gamut area of the K_2SiF_6:Mn^{4+} red phosphor. Finally, we investigate whether the light source produces under/oversaturated images or low/high fidelity images. The IES TM-30-18 Fidelity index (R_f) and the gamut index (R_g) of the fabricated LEDs are compared, as shown in Fig. 7c. The ideal value of the (R_g, R_f) is (100, 100). The deviation in the values helps us in identifying whether these LEDs generate under/oversaturated images or low fidelity images when these LEDs are used as a light source for photographic/videographic production. The LEDs exhibit low R_f while also displaying high R_g, indicating that the images reproduced using the LEDs will be slightly oversaturated and will have low fidelity.

4. Conclusions

In summary, MGF:Mn^{4+} phosphors were synthesized by replacing a small amount of MgO with metal oxides using the solid-state method. Among the transition metal oxides, Sc_2O_3 co-doped phosphors showed better optical properties, specifically at the Sc_2O_3 molar ratio of 0.01. The IQE of the Sc-codoped MGF:Mn^{4+} was increased up to 55%, which is 1.6 times higher than that of the pristine MGF:Mn^{4+} phosphor. Sc-co-doped MGF: Mn^{4+} phosphors as well as pristine MGF: Mn^{4+} phosphors maintained excellent thermal stability even up to 200 °C. A further comparison was

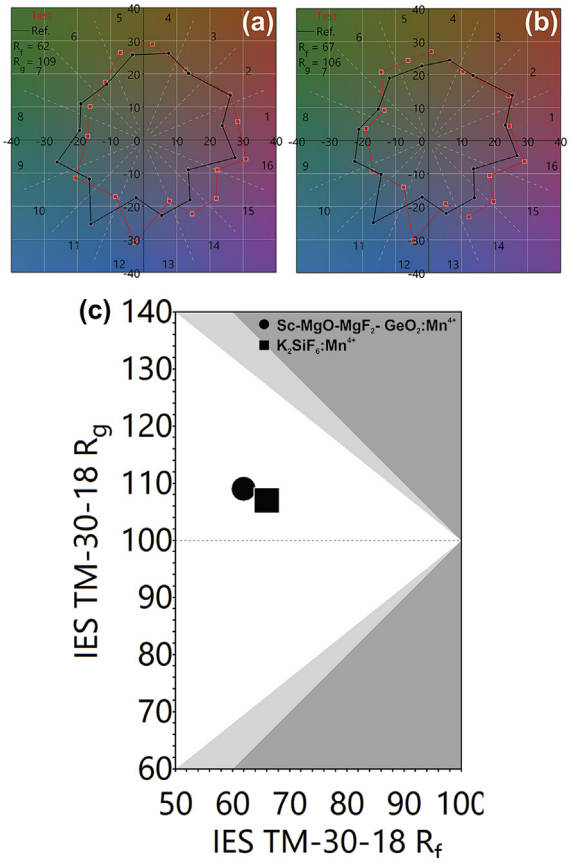

Fig. 7. Illuminating engineering society (IES) TM-30 gamut area of WLEDs fabricated using (a) β-SiAlON:Eu^{2+}(green) and Sc-MGF:Mn^{4+} (red) phosphors and (b) β-SiAlON:Eu^{2+}(green) and K_2SiF_6:Mn^{4+} (red) phosphors. (c) the R_g-R_f plot of the corresponding WLEDs. (For interpretation of the references to color in this figure legend, the reader is referred to the Web version of this article.)

conducted by fabricating white LEDs using $K_2SiF_6:Mn^{4+}$ and MGF:Mn^{4+} as red phosphors and commercial β-SiAlON:Eu^{2+} green phosphors. With respect to the coverage of color reproduction, white LEDs manufactured using the MGF:Mn^{4+} red phosphor exhibited properties superior to the NTSC, BT.2020, and IES TM-30 standards. According to the NTSC standard, there was a 3% increase in CIE 1931 and a 9% increase in CIE 1976; according to the BT.2020 standard, there was a 2% increase in CIE 1931 and a 6% increase in CIE 1976. The IES TM-30 analyses of the WLEDs fabricated using the Sc- MGF:Mn^{4+} phosphor suggests that the photographed/videographed images using these WLEDs produce slightly oversaturated and low fidelity images. The Sc-MGF:Mn^{4+} phosphor exhibits excellent potential for use in diverse LED applications. Our study provides a feasible way to enhance the IQE of Mn^{4+} activated red phosphors for use in white LED applications, and our technique can be extended to synthesize other red-emitting non-rare-earth phosphors to achieve a wider color reproduction gamut.

Declaration of competing interest

The authors declare that they have no known competing financial interests or personal relationships that could have appeared to influence the work reported in this paper.

Acknowledgments

This research was supported by the Basic Science Research Program through the National Research Foundation of Korea (NRF) funded by the Ministry of Education (No. 2018R1D1A1A02086231).

References

[1] P. Pust, P.J. Schmidt, W. Schnick, A revolution in lighting, Nat. Mater. 14 (2015) 454–458.
[2] S. Adachi, Review—Mn^{4+} -activated red and deep red-emitting phosphors, ECS J. Solid State Sci. Technol. 9 (2020), 016001.
[3] S. Li, R.-J. Xie, T. Takeda, N. Hirosaki, Critical review—narrow-band nitride phosphors for wide color-gamut white LED backlighting, ECS J. Solid State Sci. Technol. 7 (2018) R3064–R3078.
[4] Z. Xia, Z. Xu, M. Chen, Q. Liu, Recent developments in the new inorganic solid-state LED phosphors, Dalton Trans. 45 (2016) 11214–11232.
[5] K. Yoshimura, H. Fukunaga, M. Izumi, M. Masuda, T. Uemura, K. Takahashi, R.J. Xie, N. Hirosaki, White LEDs using the sharp β-sialon: Eu phosphor and Mn-doped red phosphor for wide-color gamut display applications, J. Soc. Inf. Disp. 24 (2016) 449–453.
[6] L. Wang, X. Wang, T. Kohsei, K. Yoshimura, M. Izumi, N. Hirosaki, R.-J. Xie, Highly efficient narrow-band green and red phosphors enabling wider color-gamut LED backlight for more brilliant displays, Opt. Express 23 (2015) 28707.
[7] K. Yoshimura, H. Fukunaga, M. Izumi, K. Takahashi, R.-J. Xie, N. Hirosaki, Achieving superwide-color-gamut display by using narrow-band green-emitting γ-AlON:Mn,Mg phosphor, Jpn. J. Appl. Phys. 56 (2017), 041701.
[8] P.S. Dutta, K.M. Liotta, Full spectrum white LEDs of any color temperature with color rendering index higher than 90 using a single broad-band phosphor, ECS J. Solid State Sci. Technol. 7 (2018) R3194–R3198.
[9] A.C. Duke, S. Hariyani, J. Brgoch, $Ba_3Y_2B_6O_{15}:Ce^{3+}$ - a high symmetry, narrow-emitting blue phosphor for wide-gamut white lighting, Chem. Mater. 30 (2018) 2668–2675.
[10] M.H. Fang, W.L. Wu, Y. Jin, T. Lesniewski, S. Mahlik, M. Grinberg, M.G. Brik, A.M. Srivastava, C.Y. Chiang, W. Zhou, D. Jeong, S.H. Kim, G. Leniec, S.M. Kaczmarek, H.S. Sheu, R.S. Liu, Control of luminescence by tuning of crystal symmetry and local structure in Mn^{4+} -activated narrow band fluoride phosphors, Angew. Chem. Int. Ed. 57 (2018) 1797–1801.
[11] M. Sugawara, S.Y. Choi, D. Wood, Ultra-high-definition television (Rec. ITU-R BT.2020): a generational leap in the evolution of television [standards in a nutshell], IEEE Signal Process. Mag. 31 (2014) 170–174.
[12] International Telecommunications Union, ITU. R Rec 2020, Parameter Values for Ultra-high Definition Television Systems for Production and International Programme Exchange, BT Series Broadcasting service, 2012.
[13] M.S. Jang, Y.H. Choi, S. Wu, T.G. Lim, J.S. Yoo, Material properties of the Ce^{3+}-doped garnet phosphor for a white LED application, J. Infect. Dis. 17 (2016) 117–123.
[14] G. Anoop, I.H. Cho, D.W. Suh, J.S. Yoo, Luminescence characteristics of $Sr_{1-x}Ba_xSi_2O_2N_2:Eu^{2+}$ phosphors for white light emitting diodes, Phys. Status Solidi 209 (2012) 2635–2640.
[15] G. Anoop, K.P. Kim, D.W. Suh, I.H. Cho, J.S. Yoo, Optical characteristics of $Sr_2Si_3O_2N_4:Eu^{2+}$ phosphors for white light emitting diodes, Electrochem. Solid State Lett. 14 (2011) J58.
[16] I.H. Cho, G. Anoop, D.W. Suh, S.J. Lee, J.S. Yoo, On the stability and reliability of $Sr_{1-x}Ba_xSi_2O_2N_2:Eu^{2+}$ phosphors for white LED applications, Opt. Mater. Express 2 (2012) 1292.
[17] G. Anoop, D.W. Lee, D.W. Suh, S.L. Wu, K.M. Ok, J.S. Yoo, Solid-state synthesis, structure, second-harmonic generation, and luminescent properties of non-centrosymmetric $BaSi_7N_{10}:Eu^{2+}$ phosphors, J. Mater. Chem. C. 1 (2013) 4705.
[18] G. Anoop, I.H. Cho, D.W. Suh, C.K. Kim, J.S. Yoo, Structural and luminescent characteristics of two-step processed $BaAl_{2-x}Si_xO_{4-x}N_x:Eu^{2+}$ phosphors, J. Lumin. 134 (2013) 390–395.
[19] G. Anoop, J.R. Rani, J. Lim, M.S. Jang, D.W. Suh, S. Kang, S.C. Jun, J.S. Yoo, Reduced graphene oxide enwrapped phosphors for long-term thermally stable phosphor converted white light emitting diodes, Sci. Rep. 6 (2016) 33993.
[20] T. Takeda, R.J. Xie, T. Suehiro, N. Hirosaki, Nitride and oxynitride phosphors for white LEDs: synthesis, new phosphor discovery, crystal structure, Prog. Solid State Chem. 51 (2018) 41–51.
[21] G. Li, Y. Tian, Y. Zhao, J. Lin, Recent progress in luminescence tuning of Ce^{3+} and Eu^{2+} -activated phosphors for pc-WLEDs, Chem. Soc. Rev. 44 (2015) 8688–8713.
[22] T.G. Lim, H. Jo, Y.N. Ahn, K.M. Ok, J.S. Yoo, Preparation of a $Sr_{2-x}Eu_xSi_5N_8$ phosphor using an ion transporter, ECS J. Solid State Sci. Technol. 7 (2017) R3001–R3005.
[23] T.G. Lim, Y.N. Ahn, H.W. Park, J.S. Yoo, Red-shifted absorption of a Mn^{4+} -doped germanate phosphor by crystal distortion, ECS J. Solid State Sci. Technol. 7 (2018) R3189–R3193.
[24] Y.N. Ahn, H.W. Park, T.G. Lim, J.S. Yoo, Luminescence saturation in inorganic phosphors under high flux of photon excitation, ECS J. Solid State Sci. Technol. . 7 (2018) R104–R110.
[25] J. Li, J. Yan, D. Wen, W.U. Khan, J. Shi, M. Wu, Q. Su, P.A. Tanner, Advanced red phosphors for white light-emitting diodes, J. Mater. Chem. C. 4 (2016) 8611–8623.
[26] H. Zhu, C.C. Lin, W. Luo, S. Shu, Z. Liu, Y. Liu, J. Kong, E. Ma, Y. Cao, R.S. Liu, X. Chen, Highly efficient non-rare-earth red emitting phosphor for warm white light-emitting diodes, Nat. Commun. 5 (2014) 4312.
[27] H.F. Sijbom, R. Verstraete, J.J. Joos, D. Poelman, P.F. Smet, $K_2SiF_6:Mn^{4+}$ as a red phosphor for displays and warm-white LEDs: a review of properties and perspectives, Opt. Mater. Express 7 (2017) 3332.
[28] S. Adachi, Photoluminescence properties of Mn^{4+}-activated oxide phosphors for use in white-LED applications: a review, J. Lumin. 202 (2018) 263–281.
[29] Q. Huang, W. Ye, G. Hu, X. Jiao, X. Liu, Deep red emission enhancement in $Mg_{28}Ge_{10}O_{48}:Mn^{4+}$ phosphor by Zn substitution, J. Lumin. 194 (2018) 557–564.
[30] M. Zhu, Y. Pan, L. Xi, H. Lian, J. Lin, Design, preparation, and optimized luminescence of a dodec-fluoride phosphor $Li_3Na_3Al_2F_{12}:Mn^{4+}$ for warm WLED applications, J. Mater. Chem. C. 5 (2017) 10241–10250.
[31] L.-L. Wei, C.C. Lin, M.-H. Fang, M.G. Brik, S.-F. Hu, H. Jiao, R.-S. Liu, A low-temperature co-precipitation approach to synthesize fluoride phosphors $K_2MF_6:Mn^{4+}$ (M = Ge, Si) for white LED applications, J. Mater. Chem. C. 3 (2015) 1655–1660.
[32] Z. Zhou, N. Zhou, M. Xia, M. Yokoyama, H.T. Hintzen, Research progress and application prospects of transition metal Mn^{4+} -activated luminescent materials, J. Mater. Chem. C. 4 (2016) 9143–9161.
[33] E. Song, Y. Zhou, X.-B. Yang, Z. Liao, W. Zhao, T. Deng, L. Wang, Y. Ma, S. Ye, Q. Zhang, Highly efficient and stable narrow-band red phosphor $Cs_2SiF_6:Mn^{4+}$ for high-power warm white LED applications, ACS Photonics 4 (2017) 2556–2565.
[34] J. Zhong, X. Chen, D. Chen, M. Liu, Y. Zhu, X. Li, Z. Ji, A novel rare-earth free red-emitting $Li_3Mg_2SbO_6:Mn^{4+}$ phosphor-in-glass for warm w-LEDs: synthesis, structure, and luminescence properties, J. Alloy. Comp. 773 (2019) 413–422.
[35] Q. Zhou, L. Dolgov, A.M. Srivastava, L. Zhou, Z. Wang, J. Shi, M.D. Dramićanin, M.G. Brik, M. Wu, Mn^{2+} and Mn^{4+} red phosphors: synthesis, luminescence and applications in WLEDs. A review, J. Mater. Chem. C. 6 (2018) 2652–2671.
[36] M. Zhu, Y. Pan, M. Wu, H. Lian, J. Lin, Optimized photoluminescence properties of a novel red phosphor $LiSrAlF_6:Mn^{4+}$ synthesized at room-temperature, J. Alloy. Comp. 774 (2019) 331–337.
[37] Y. Wu, Y. Zhuang, Y. Lv, K. Ruan, R.-J. Xie, A high-performance non-rare-earth deep-red-emitting $Ca_{14-x}Sr_xZn_6Al_{10}O_{35}:Mn^{4+}$ phosphor for high-power plant growth LEDs, J. Alloy. Comp. 781 (2019) 702–709.
[38] J.Y. Park, J.S. Joo, H.K. Yang, M. Kwak, Deep red-emitting $Ca_{14}Al_{10}Zn_6O_{35}:Mn^{4+}$ phosphors for WLED applications, J. Alloy. Comp. 714 (2017) 390–396.
[39] L. Sun, B. Devakumar, J. Liang, S. Wang, Q. Sun, X. Huang, Simultaneously enhanced far-red luminescence and thermal stability in $Ca_3Al_4ZnO_{10}:Mn^{4+}$ phosphor via Mg^{2+} doping for plant growth lighting, J. Alloy. Comp. 785 (2019) 312–319.
[40] Q. Shao, L. Wang, L. Song, Y. Dong, C. Liang, J. He, J. Jiang, Temperature dependence of photoluminescence spectra and dynamics of the red-emitting $K_2SiF_6:Mn^{4+}$ phosphor, J. Alloy. Comp. 695 (2017) 221–226.
[41] T. Deng, E. Song, Y. Zhou, J. Yuan, Implementation of high color quality, high luminous warm WLED using efficient and thermally stable $Rb_3AlF_6:Mn^{4+}$ as red color converter, J. Alloy. Comp. 795 (2019) 453–461.
[42] L. Zhou, C. Shen, L. Shen, S. Liu, J. Liu, L. Ding, J. Du, W. Xiang, X. Liang, Enhanced luminescence performances of $Mn^{4+}:Y_3Al_5O_{12}$ red phosphor by ions of Rn^{2+} (Be^{2+}, Mg^{2+}, Sr^{2+}, Ba^{2+}), J. Alloy. Comp. 769 (2018) 686–693.

[43] H. Jia, L. Cao, Y. Wei, H. Wang, H. Xiao, G. Li, J. Lin, A narrow-band red-emitting $K_2LiGaF_6:Mn^{4+}$ phosphor with octahedral morphology: luminescent properties, growth mechanisms, and applications, J. Alloy. Comp. 738 (2018) 307–316.
[44] L. Qin, S. Bi, P. Cai, C. Chen, J. Wang, S. Il Kim, Y. Huang, H.J. Seo, Preparation, characterization and luminescent properties of red-emitting phosphor: $LiLa_2NbO_6$ doped with Mn^{4+} ions, J. Alloy. Comp. 755 (2018) 61–66.
[45] C. Zheng, L. Meng, J. Chen, F. Lu, L. Zhang, Q. Pang, L. Liang, Sol-gel derived Mn^{4+}-activated magnesium fluorogermanate nanosized phosphors with deep-red emission properties, Opt. Mater. 36 (2014) 1859–1864.
[46] L. Peng, W. Chen, S. Cao, B. Liu, T. Han, L. Zhao, C. Zhao, F. Li, X. Li, Enhanced photoluminescence and thermal properties due to size mismatch in $Mg_2Ti_xGe_{1-x}O_4:Mn^{4+}$ deep-red phosphors, J. Mater. Chem. C. 7 (2019) 2345–2352.
[47] H. Liao, M. Zhao, Y. Zhou, M.S. Molokeev, Q. Liu, Q. Zhang, Z. Xia, Polyhedron transformation toward stable narrow-band green phosphors for wide-color-gamut liquid crystal display, Adv. Funct. Mater. 29 (2019) 1901988.
[48] S. Okamoto, H. Yamamoto, Luminescent-efficiency improvement by alkaline-earth fluorides partially replacing MgO in $3.5MgO{\cdot}0.5MgF_2{\cdot}GeO_2:Mn^{4+}$ deep-red phosphors for light emitting diodes, J. Electrochem. Soc. 157 (2010) 59–63.
[49] J.W. Moon, B.G. Min, J.S. Kim, M.S. Jang, K.M. Ok, K.-Y. Han, J.S. Yoo, Optical characteristics and longevity of the line-emitting $K_2SiF_6:Mn^{4+}$ phosphor for LED application, Opt. Mater. Express 6 (2016) 782.
[50] Z. Hou, X. Tang, X. Luo, T. Zhou, L. Zhang, R.-J. Xie, A green synthetic route to the highly efficient $K_2SiF_6:Mn^{4+}$ narrow-band red phosphor for warm white light-emitting diodes, J. Mater. Chem. C. 6 (2018) 2741–2746.
[51] A. V Shamshurin, N.P. Efryushina, A.V. Repin, Mn^{4+} luminescence in $2MgO{\cdot}GeO_2$ and $2MgO{\cdot}GeO_2{\cdot}MgF_2$, Inorg. Mater. 36 (2000) 629–631.
[52] M. Royer, Evaluating Color Rendering with TM-30, 2016.
[53] A. David, P.T. Fini, K.W. Houser, Y. Ohno, M.P. Royer, K.A.G. Smet, M. Wei, L. Whitehead, Development of the IES method for evaluating the color rendition of light sources, Opt. Express 23 (2015) 15888.